On optimal optical properties for near-eld radiative heat transfer maximization between two semi-innite planes at room tempertature

E. Nefzaoui, Younes Ezzahri, Jérémie Drevillon, Karl Joulain

Proceedings of the 7^{th} International Symposium on Radiative Transfer, RAD-13
June 2-8, 2013, Kuşadasi, Turkey

RAD-13-XXX

On optimal optical properties for near-field radiative heat transfer maximization between two semi-infinite planes at room tempertature

Elyes NEFZAOUI, Younès EZZAHRI, Jérémie DREVILLON and Karl JOULAIN
Institut Pprime, CNRS-Université de Poitiers-ENSMA, Département Fluides, Thermique, Combustion, ENSIP-Bâtiment de mécanique, 2, Rue Pierre Brousse, F 86022 Poitiers, Cedex, France

ABSTRACT. A parametric study of Drude and Lorentz models performances in maximizing near-field radiative heat transfer between two semi-infinite planes separated by nanometric distances at room temperature is presented in this paper. Optimal parameters of these models that provide optical properties maximizing the radiative heat flux are reported and compared to real materials usually considered in similar studies, silicon carbide and heavily doped silicon in this case. Results are obtained by exact and approximate (in the extreme near-field regime and the electrostatic limit hypothesis) calculations. The two methods are compared in terms of accuracy and CPU resources consumption. Finally, the frequently assumed hypothesis which states a maximal transfer when the two semi-infinite planes are of identical materials is numerically confirmed. Its subsequent practical constraints are then discussed.

NOMENCLATURE

*

Greek letters

ϵ	Dielectric permittivity
Γ	Damping factor
γ	Normal wave vector component
ω_0	Transverse optical phonons circular frequency (also usually referred to by ω_{TO})
ω_p	Plasma frequency
ω_{LO}	Longitudinal optical phonons circular frequency
Θ	Planck oscillator energy

Latin letters

$\mathbf{q}$	Transverse wave vector component
g_0	Quantum of heat conduction
n	Mesh points number
r_{3j}	Fresnel reflexion coefficient between media 3 and j
u	Reduced frequency

Subscripts

∞ High frequency limit

evan Evanescent waves contribution

j Medium number, $j \in \{1, 2\}$

prop Propagative waves contribution

Superscripts

i Wave polarization, $i \in \{s, p\}$

INTRODUCTION

It has been shown in the late 1960 [1, 2] that the radiative heat flux (RHF) exchanged by two media in the near-field (NF), i.e. when these media are separated by very small distances (smaller than the thermal radiation characteristic wavelength) could exceed by several orders of magnitude the black body limit. This topic has then received an increasing attention until its recent experimental verifications [3, 4, 5]. Experiments exclusively focused on asymmetric configurations such as plane-tip or plane-sphere configurations. On the other hand, the symmetric plane-plane configuration, potentially useful for various applications such as the cooling of high flux density electronic devices [6] or thermo-photovoltaic (TPV) conversion of radiative energy [7], has been thoroughly investigated from a theoretical point of view by several groups. These theoretical works mainly addressed dielectrics, usually silicon carbide (SiC) [8, 9] which surface phonon-polaritons highly contribute to the NF RHF increase. They also considered materials which support plasmon-polaritons in the wavelength range of thermal radiation at room temperature such as tungsten [10, 11] or heavily doped silicon (HD-Si) [12, 13].
In the present numerical work, hypothetic materials modeled by Drude and Lorentz models are considered. The aim of this work is to find the sets of parameters of these models that possibly maximize the RHF between two semi-infinite planes of identical materials separated by a nonometric gap at room temperature. For this purpose, we calculate the exchanged RHF between the two media while varying the different parameters in a wide range. Exact and approximate calculations are performed and their accuracy/resources consumption ratio compared. Then, the optimal hypothetical material performances are compared to those of usually considered materials, SiC and HD-Si for instance. Finally, the influence of small discrepancies between the optical properties of the two planes on the exchanged RHF is discussed.

FORMALISM

The two methods used to calculate NF RHF between two semi-infinite planes and to obtain results presented later in this paper are briefly reminded in this section.

Exact calculation

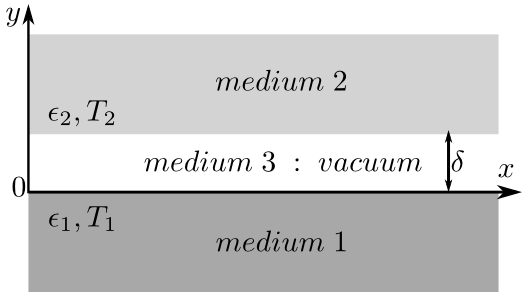

Figure 1: Two semi-infinite planes separated by a distance δ.

Consider two semi-infinite planes 1 and 2 separated by a gap of thickness δ (Figure 1) and characterized by their dielectric functions and temperatures (ϵ_1, T_1) and (ϵ_2, T_2) respectively. The total RHF density exchanged by the two media is given by [14]:

$$\dot{q} = \dot{q}_{prop} + \dot{q}_{evan} \tag{1}$$

where

$$\dot{q}_{prop} = \sum_{i=s,p} \int_0^\infty \frac{d\omega}{2\pi} [\Theta(\omega, T_1) - \Theta(\omega, T_2)] \int_0^{\frac{\omega}{c}} \frac{d^2q}{(2\pi)^2} \frac{(1-|r_{31}^i|^2)(1-|r_{32}^i|^2)}{|1 - r_{31}^i r_{32}^i e^{2\imath\gamma_3\delta}|^2} \tag{2}$$

and

$$\dot{q}_{evan} = \sum_{i=s,p} 4 \int_0^\infty \frac{d\omega}{2\pi} [\Theta(\omega, T_1) - \Theta(\omega, T_2)] \int_{\frac{\omega}{c}}^\infty \frac{d^2q}{(2\pi)^2} e^{2\imath\gamma_3\delta} \frac{\mathrm{Im}(r_{31}^i)\,\mathrm{Im}(r_{32}^i)}{|1 - r_{31}^i r_{32}^i e^{2\imath\gamma_3\delta}|^2} \tag{3}$$

are the contributions of propagative and evanescent waves respectively.

$$\Theta(\omega, T) = \frac{\hbar\omega}{e^{\frac{\hbar\omega}{kT}} - 1} \tag{4}$$

is the mean energy of a Planck oscillator at a temperature T. r_{3j}^i are Fresnel reflection coefficients for an i-polarized wave ($i \in \{s, p\}$) propagating from medium 3 to medium j. γ_3 is the wave vector normal component in medium 3 and is given by:

$$\gamma_3 = \sqrt{\left(\frac{\omega}{c}\right)^2 - q^2} \tag{5}$$

where $\mathbf{q}$ is the component of the wave vector parallel to the interfaces. Expressions 2 and 3 express the total heat flux as the sum of the energy of different existing oscillators at a temperature T, transported by different modes $(\omega, \mathbf{q})$. It is worth noting that for $q > \frac{\omega}{c}$, γ_3 is imaginary, the corresponding waves are evanescent and their magnitude decreases when going away from the surface. Corresponding modes are surface waves modes.
To obtain the total heat flux, a double integration over all modes $(\omega, \mathbf{q})$ is to be made. Its calculation may prove to be very resource-consuming since the cutoff wave vector q_c for the integral over q is not known a priori. Different authors have proposed different approximations for the cutoff wave vector : $q_c = 1/\delta$ [13, 15], $q_c = \sqrt{4/\delta^2 + (\omega/c)^2}$ [16] and $q_c = 1/a$ [17] where a denotes the lattice constant of the considered material. In this work, $q_c = 50/\delta$ is adopted.

Approximate calculation Recently, Rousseau et al. [13, 18, 9] derived, under few simple conditions, an asymptotic expression of the NF RHF p-polarized evanescent contribution. This contribution is considered for two reasons. First, it dominates the other contributions in extreme near-field regime for dielectrics and some other materials such as HD-Si for instance. Second, its exact calculation is the most resource-consuming due to the unknown and eventually large cutoff wave vector in some situations.
First, they started, when considering a small temperature difference δT between the two planes, by defining a radiative NF exchange coefficient h :

$$h = \frac{\dot{q}(\delta, T)}{\delta T} \tag{6}$$

which can be written as the sum of two coefficients h_{prop} and h_{evan} corresponding to the propagative and evanescent contributions respectively. Let's focus on the i-polarized ($i \in \{p, s\}$)

evanescent contribution monochromatic exchange coefficient which is given by :

$$h^i_{evan}(\omega) = \left[\int_{\frac{\omega}{c}}^{\infty} \frac{d^2q}{(2\pi)^2}\left(4\times e^{2\imath\gamma_3\delta}\frac{\mathrm{Im}(r^i_{31})\,\mathrm{Im}(r^i_{32})}{|1-r^i_{31}r^i_{32}e^{2\imath\gamma_3\delta}|^2}\right)\right]\times\frac{\partial\Theta(\omega,T)}{\partial T} \quad (7)$$

$$= 2\pi h^0(\omega,T)\times\int_{\frac{\omega}{c}}^{\infty}\frac{qdq}{q_0^2}\tau^i_{evan}(r^i_{3j},\delta) \quad (8)$$

where $\tau^i_{evan}(r^i_{3j},\delta)$ is $(\omega,\mathbf{q})$ mode transmission probability from medium 1 to medium 2 and

$$h^0(\omega,T) = \frac{q_0^2}{4\pi^2}\frac{\partial\Theta}{\partial T} \quad (9)$$

$$= \frac{1}{T}\frac{\hbar\omega}{kT}\frac{\hbar\omega^3}{4\pi^2c^3}\left(\frac{1}{2\ \sinh(\frac{\hbar\omega}{2kT})}\right)^2 \quad (10)$$

is proportional to Planck function derivative. If we consider the electrostatic regime, i.e. $q\gg q_0=\frac{\omega}{c}$, p-polarization Fresnel coefficients become independent of q since they tend toward $r^p=\frac{\epsilon-1}{\epsilon+1}$. Then, we can show [9] that h^p_{evan}, prevailing in our case, may be written :

$$h^p_{evan}(u,T,\delta) = \frac{3}{2\pi^3}\frac{g_0}{d^2}h^0(u)\times\frac{\mathrm{Im}(r^p_{31})\,\mathrm{Im}(r^p_{32})}{\mathrm{Im}(r^p_{31}r^p_{32})}\,\mathrm{Im}(Li_2(r^p_{31}r^p_{32})) \quad (11)$$

where Li_2 is the dilogarithm function (see [19] for definition and [20] for numerical evaluation), $h^0(u)=\frac{u^2}{(e^u-1)^2}$, $u=\frac{\hbar\omega}{kT}$ and $g_0=\frac{\pi^2k^2T}{3h}$ is the quantum of heat conduction.
NF heat flux is then given by :

$$\dot{q}(T,\delta) \simeq \left(\int_0^{\infty} h^p_{evan}(u,T,\delta)du\right)\times\delta T \quad (12)$$

Therefore, the heat flux calculation is reduced to a simple integral evaluation and the problem of the cutoff wave vector is apparently resolved. Given the assumed hypotheses in order to obtain expressions 11 and 12, a verification with an exact calculation of results obtained by this method might be necessary.

OPTIMIZATION STATE OF THE ART

Different groups have already tackled the question of maximizing the NF radiative heat transfer, for plane-plane configuration in particular. Zhuoming Zhang's group of Georgia Tech. has been particularly prolific. First, Basu et al. [21] lead a theoretical parametric study of radiative transfer between two semi-infinite planes of HD-Si. This material was considerd because of its interesting optical properties that can be controlled through the doping level [21, 22, 23].In fact, its dielectric permittivity is modeled by a Drude model where the doping concentration controls both of the plasma frequency ω_p and the damping coefficient Γ. They observed that the RHF spectrum presents a peak around the plasma frequency and a blue-shift of the peak position when the doping concentration increases. They also note that the total exchanged RHF increases with doping until a maximum that depends on temperature and ω_p. At room temperature, this optimum is observed for a doping concentration between 10^{19} and 10^{20} (cm^{-3}). Let us note that similar results, obtained by a different approach, have been reported by another group for HD-Si [13]. Finally, they considered two planes with different doping concentrations and tend towards the conclusion that the maximal RHF is obtained for identical media. Then, in another work [24], they went beyond the particular case of HD-Si by considering two identical semi-infinite planes of a completely fictive material. They observed that the dieletric

permittivity maximizing the exchanged RHF can be written $\epsilon = -1 + \imath\delta$ with $\mathrm{Im}(\epsilon) = \delta \ll 1$. It is worth noting here that this form of ϵ underlies a hypothesis of a non-dispersive medium. At the same time, Wang et al. [17] considered less restrictive situations and generalized first results previously obtained for HD-Si to other real materials (SiC, MgO) and fictive materials modeled by Drude and Lorentz models. For Drude model, control parameters are ω_p and Γ and the high frequency limit of the dielectric permittivity ϵ_∞. Lorentz model has an additional parameter ω_0 which corresponds to the frequency of transverse optical phonons. Authors make the following general conclusions : (1) Drude model leads to higher values of maximal RHF than Lorentz model. For this reason, Lorentz model presents its highest preformances when $\omega_0 = 0$, i.e. when it is equivalent to Drude model. That is why we focus on Drude model in the following points. (2) For Drude model : (2-1) Lower values of ϵ_∞ lead to the higher values of maximal RHF. These values are the closest to the condition given by [24] and previously presented. (2-2) At room temperature, a maximum of RHF is observed for $\omega_p \simeq 10^{14}$ (rad.s^{-1}) and $\Gamma/\omega_p \simeq 0,1$. The position of this maximum is strongly T-dependent. In addition, the maximum is realized by a compromise between the peak width (controlled by Γ) and the peak position (controlled by ω_p).

More recently, several authors exploited graphene features to enhance NF RHF. Graphene presents palsmon-polaritons in the terahertz domain which makes it particularly interesting for radiative heat transfer around room temperature[25]. Besides, more than HD-Si, its optical properties can be tuned with doping level or chemical potential. Finally, graphene dielectric function is non-local, i.e. its dielectric permittivity in general, and its plasma frequency in particular, depend on the wave vector. Therefore, it presents a big variety of resonant modes which may allow to consider their coupling with other materials resonant modes. These authors showed that a thin film of graphene deposited on a dielectric that does not support surface phonon-polaritons leads to an enhancement of the exchanged NF RHF between two semi-infinite planes of the same graphene-covered material by three and almost four orders of magnitude. However, this enhancement decreases rapidly with temperature and is spectacular only for temperatures lower than room temperature. An other group from l'Institut d'Optique [26], showed for a plane-plane system of SiC, that a thin film of graphene on the surface of one of the two planes leads to additional peaks in the spectrum of the local density of states due to the coupling of graphene modes with those of SiC. These modes contribute to the increase of exchanged NF RHF.

Shall we here emphasize practical potential of graphene as a selective emitter for NF TPV devices. Indeed, the possibility to tune graphene plasmon-polariton resonance frequencies would allow their adjustment to the band gap of different photovoltaic converters. Messina et al. actually demonstrated [27] for a TPV device composed of a boron nitride emitter (at $T_e = 450$ K) and an indium antimonide cell, that a graphene film with a chemical potential of 0.5 eV on the surface of the cell leads to an increase of the maximal efficiency of the system by a factor two to reach $\eta \simeq 20\%$ and an increase of output power by almost one order of magnitude. Higher performances corresponding to higher operating temperatures in the range $[600, 1200]$ K have been recently presented by an other group of the MIT [28] who considered a slightly different system where graphene plays the role of a selective emitter. Prior works had already considered NF TPV devices based on metallic selective emitters such as tungsten [10, 11, 7] but graphene seems to monopolize the community recent attention due to the diversity of potential applications it makes possible thanks to the "flexibility" of its surface modes and optical properties.

RESULTS

Formalisms presented in the first section are used to calculate exchanged NF RHF between two semi-infinite planes separated by a distance $\delta = 10$ nm. Planes dielectric functions are

modeled by local (gap thickness considered here is much larger than non-local phenomena onset distances [29, 30]) Drude and Lorentz models usually adopted to describe real materials. Calculations are made for both identical and different planes around 300 K while varying models parameters in their usual variation ranges with three main goals in mind : (1) For identical planes : to determine optical properties, fictive in this case, that would maximize NF RHF in order to guide, for a given application, the choice of a real material to use or the design of meta-materials (2) For different planes : to verify the hypothesis which states that the maximal RHF is obtained when the two planes materials are identical (3) To compare the accuracy and the resource-consumption cost of the exact and approximate methods.

Drude model We remind the expression of the dielectric permittivity in this model :

$$\epsilon(\omega) = \epsilon_\infty - \frac{\omega_p^2}{\omega^2 + \imath\Gamma\omega} \tag{13}$$

where ϵ_∞ is the high frequency limit of the dielectric permittivity, ω_p the plasma frequency and Γ the damping coefficient.

Identical media
First, we calculate NF RHF between two identical semi-infinite planes modeled by Drude model with $\epsilon_\infty = 1$. ω_p and Γ are varied within the ranges $[10^{13}, 10^{15}]$ and $[10^{-2} \times \omega_p, 10 \times \omega_p]$ respectively which cover these parameters ranges for HD-Si. Some values of these parameters for HD-Si with doping concentration around 10^{19} cm^{-3} are given in Table 1. Media 1 and 2 are

N°	Doping type	Concentration $\times 10^{-19}(cm^{-3})$	ϵ_∞	$\omega_p \times 10^{-14}$ (rad.s^{-1})	$\frac{\Gamma}{\omega_p}$
1	Si:B	27	11.8	16	6.7×10^{-1}
2	Si:B	6.7	11.8	8.3	1.7×10^{-1}
3	Si:P	10	11.8	9.7	5.1×10^{-1}
4	Si:P	5.3	11.8	7.28	10^{-1}
5	Si:P	1.6	11.8	4	1.3×10^{-1}
6	Si:P	0.52	11.8	2.3	6×10^{-2}

Table 1: Drude model parameters for the dielectric permittivity of p and n-type HD-Si with bore (Si:B) and phosphorus (Si:P) respectively [31].

considered at 300 K and 299 K respectively.

Plasma frequency and damping effects We present in figure 2 the normalized RHF exchanged between the two media. Plotted results are obtained by both exact calculation (Figure 2a) and asymptotic calculation in the case of extreme NF with the electrostatic approximation (Figure 2b). Only the dominating p-polarization is presented here. First, we can note the actual existence of a maximum (See Table 2 for its value and coordinates.). Beyond the maximum position, these figures reveal the RHF sensitivity to the different parameters. In fact, we observe that a relative variation between 22% and 27% for ω_p and of about 50% for Γ gives values of the flux larger than $0.95 \times \dot{q}_{max}$. These parameters values admissible variations to keep high flux values are slightly larger than those reported in literature [12].

High frequency limit of the dielectric permittivity effect Similar calculation results are presented in Figure 3 for $\epsilon_\infty = 5$ (Figures 3b and 3a) and $\epsilon_\infty = 10$ (figures 3d and 3c). We observe as Basu et al.[12], a decrease of the maximal flux value when ϵ_∞ increases. In fact, lower values of ϵ_∞ lead to lower values of $\mathrm{Re}(\epsilon) = \epsilon_\infty - \mathrm{Re}(\frac{\omega_p^2}{\omega^2+\imath\Gamma\omega})$ which are the closet to fit Basu et al. condition to maximize the NF RHF[24], i.e. $\mathrm{Re}(\epsilon) = -1$.

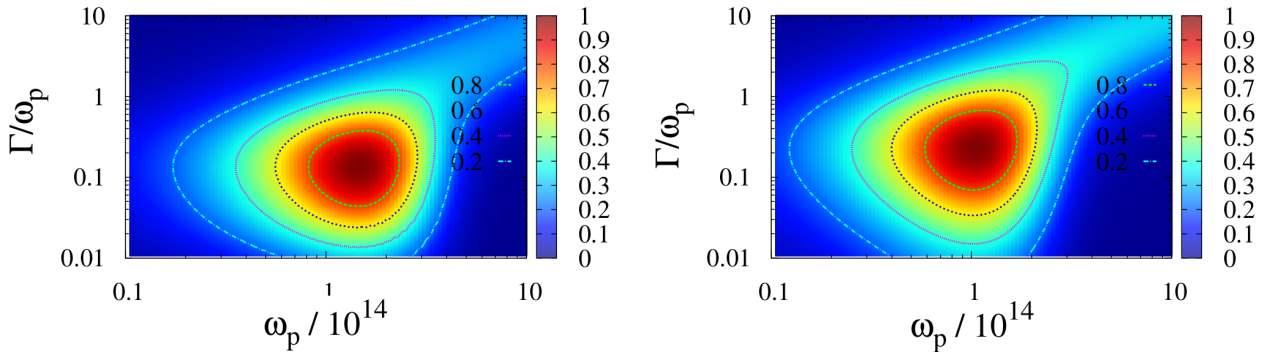

(a) (b)

Figure 2: Normalized NF RHF between two identical semi-infinite planes. The dielectric permittivity is given by Drude mode with $\epsilon_\infty = 1$. Results are obtained by both exact calculation (a) and asymptotic one (b).

Method	ϵ_∞	$\omega_p \times 10^{-14}$ (s^{-1})	$\frac{\gamma}{\omega_p}$	$\dot{q}_{max}$ (W.m^{-2})	$n_{\omega,q}$	$n_{\omega_p,\Gamma}$	t (s)
E	1	1.51	0.17	229336	500	100	32921
A	1	1.05	0.24	229208	1000	100	23
E	5	2.51	3.7×10^{-2}	78656	500	100	14864
A	5	0.79	0.11	78676	1000	100	13
E	10	3.47	1.51×10^{-2}	42123	400	100	13952
A	10	0.76	6.91×10^{-2}	43128	1000	100	13
E	20	4.57	2.29×10^{-3}	24269	400	100	16961
A	20	0.72	3.71×10^{-2}	22621	1000	100	13

Table 2: Drude model parameters maximizing the exchanged NF RHF between two semi-infinite planes separated by a gap of thickness $\delta = 10$ nm for different values of ϵ_∞. Values are obtained by both exact (E) and approximate (A) calculations. $n_{\omega,q}$ and $n_{\omega_p,\Gamma}$ are mesh points numbers for (ω,q) modes and for control parameters (ω_p and Γ) respectively. t is CPU calculation time to obtain the corresponding figures.

Exact versus approximate calculation Maximal values of the RHF obtained by both methods are almost the same with a relative error around 10^{-4} (see Table 2). In the case $\epsilon_\infty = 1$, maxima are realized for $(\omega_p, \frac{\Gamma}{\omega_p}) = (1.51 \times 10^{14}\ rad.s^{-1}, 1.7 \times 10^{-1})$ and $(\omega_p, \frac{\Gamma}{\omega_p}) = (1.05 \times 10^{14}\ rad.s^{-1}, 0.24 \times 10^{-1})$ with exact and approximate calculations respectively. The relative error on positions is quite important, up to 27% and 82% for ω_p and Γ respectively. An exact calculation of the flux value corresponding to approximate optimal parameters is 30% lower than the actual maximal flux value. This discrepancy on optimal parameters given by both methods increases with ϵ_∞. Let us note however the resource-consumption gain made by the use of the asymptotic approximation : figure 2a (exact) was obtained in 32921 (s) versus 23 (s) for figure 2b (approximate), i.e. a ratio of almost 1500 between the two. This ratio particularly depends on the parallel wave vector mesh resolution and increases rapidly with it. Calculations were made on an Intel® Xeon® E5620 @ 2.40GHz, with 12288 Kb of cache and 4 Go of RAM memory.

Case of heavily doped silicon at 300 K Figure 4 presents similar results for $\epsilon_\infty = \epsilon_{\infty,Si} = 11.8$. The aim here is to determine whether HD-Si, previously considered by several authors[12, 13] to maximize NF RHF, is well adapted to this task. For this reason, parameters values corresponding to HD-Si are represented on the same figure by crosses. Previously reported results [12, 13] stating a maximal flux for a doping concentration between 10^{19} and

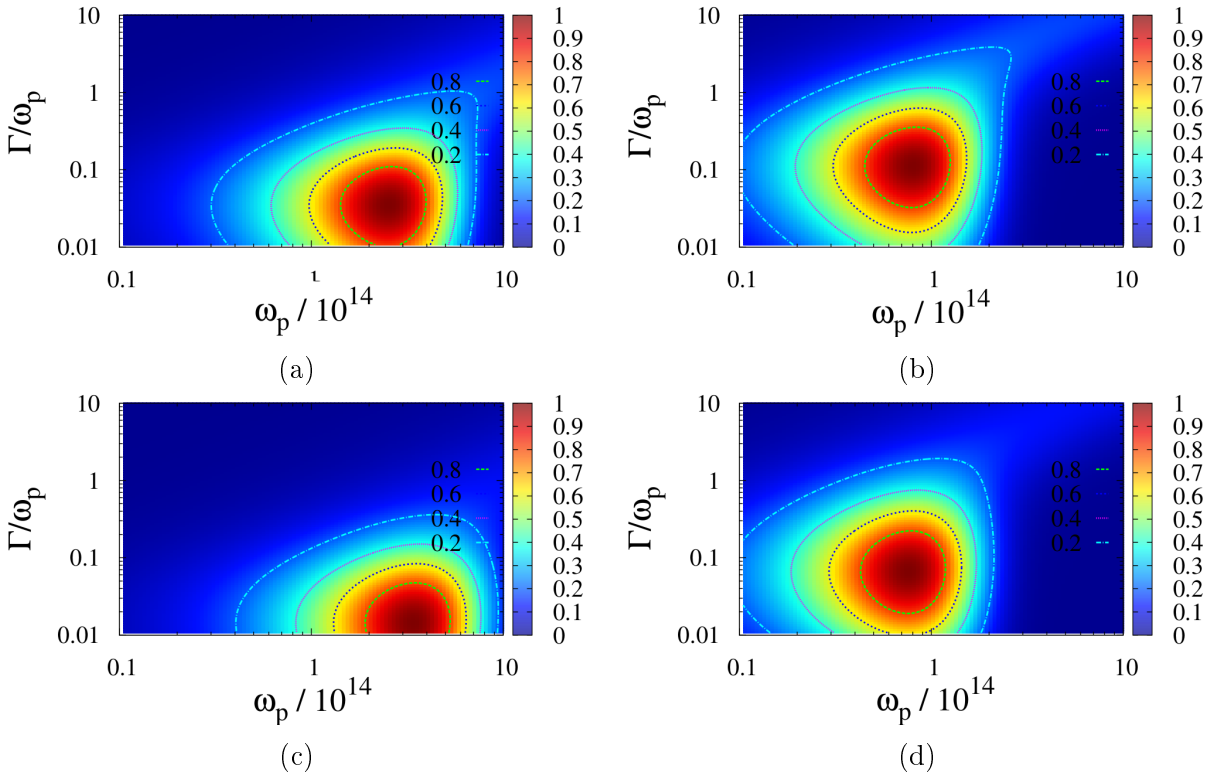

Figure 3: Normalized NF RHF between two semi-infinite planes modeled by Drude model for $\epsilon_\infty = 5$: (a - b) and $\epsilon_\infty = 10$: (c - d) obtained by exact (left column) and approximate (right column) calculations.

10^{20} (cm^{-3}) are more likely to be confirmed. Besides, we can state according to this figure that HD-Si around 10^{19} (cm^{-3}) is a good candidate to NF RHF maximization at room temperature since it allows to reach almost $0.9 \times \dot{q}_{max}$ that can be obtained with a Drude model with $\epsilon_\infty = 11.8$ (we obviously assume that ϵ_∞ is a parameter that can hardly be varied).

Non-identical media

The only change considered in this paragraph lies in the fact that exchanging semi-infinite planes dielectric functions are not identical while they are still modeled by a Drude model. We are aiming to a double objective : (1) verify the statement of maximal flux for identical media due to a more efficient coupling of identical modes supported by the same materials (2) See in what extent, a more or less important difference in optical properties of considered materials affects the exchanged NF RHF. This second objective has an obvious applied interest since real materials eventually used in a particular application are never exactly identical. For this sake, we consider the two media around 300 K separated by $\delta = 10$ nm. We also consider, without generality loss, $\epsilon_\infty = 1$. Medium 1 parameters are fixed to optimal values previously obtained (Table 2, line 1). Control parameters are then the second medium Drude model parameters, i.e. $\omega_{p,2}$ and Γ_2. Figure 5 presents the normalized exchanged NF RHF as a function of plasma frequencies ratio $\omega_{p,2}/\omega_{p,1}$ and damping factors ratio Γ_2/Γ_1.
The maximum is actually realized for $(\omega_{p,2}/\omega_{p,1}, \Gamma_2/\Gamma_1) = (1, 1)$, i.e. for identical media. Besides, the flux value is more sensitive to ω_p than to Γ value. In fact, the flux is maintained at high values ($\dot{q} > 0.9 \times \dot{q}_{max}$) for $\omega_{p,2}/\omega_{p,1} \in [0.9, 1.1]$ and $\Gamma_2/\Gamma_1 \in [0.49, 2.53]$. A 10% variation of ω_p leads to a comparable variation of the flux value. The same flux variation is obtained with a variation of Γ up to 150%. However, the asymmetry of $\dot{q}$-behavior as a function of Γ is

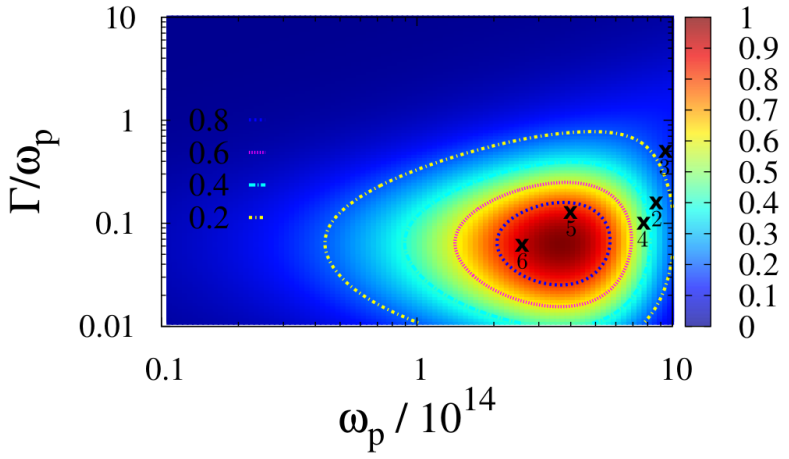

Figure 4: Normalized NF RHF for $\epsilon_\infty = \epsilon_{\infty,Si} = 11.8$. Crosses represent p and n-type HD-Si at different doping concentrations (see Table 1 for parameters values of the different points).

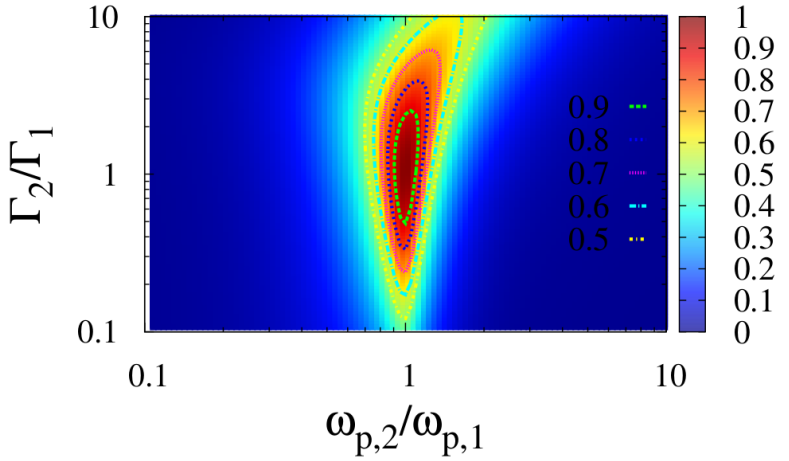

(a)

Figure 5: NF RHF exchanged by two semi-infinite planes of different optical properties modeled by Drude model function of plasma frequencies ratio and damping factors ratio obtained by exact calculation.

worth noting. In fact, the sign of Γ-variation affects strongly the variation of the flux. Finally, the flux sensitivity to ω_p decreases for larger values of Γ. This is due to the fact that Γ controls the exchanged flux spectral density peak width [12] : the larger Γ the larger the peak width which allows looser constraints on the peak position controlled by ω_p.

Lorentz model First, we remind the dielectric permittivity expression according to this model[32] :

$$\epsilon(\omega) = \epsilon_\infty - \frac{\omega_p^2}{\omega^2 + \imath\Gamma\omega - \omega_0^2} \tag{14}$$

where $\omega_p^2 = \omega_{LO}^2 - \omega_0^2$ with ω_{LO} the longitudinal optical phonons circular frequency, $\omega_0 = \omega_{TO}$ the transverse optical phonons circular frequency and Γ the damping factor.

Identical media

First, identical media are considered, medium 1 at 300 K and medium 2 at 299 K. The gap thickness between the two planes is $\delta = 10$ nm. Compared to Drude model, Lorentz model has

an additional parameter, transverse optical phonons frequency ω_0 in this case. In this study, $\omega_0 = \omega_{0,SiC} = 1.49 \times 10^{14}$ (rad.s^{-1}) [32] is considered constant which reduces the problem to a two-parameter problem. Control parameters are ω_{LO} and Γ. Results will be presented as a function of $\frac{\omega_{LO}}{\omega_0}$ and $\frac{\Gamma}{\omega_0}$.

Longitudinal phonons frequency and damping factor effect

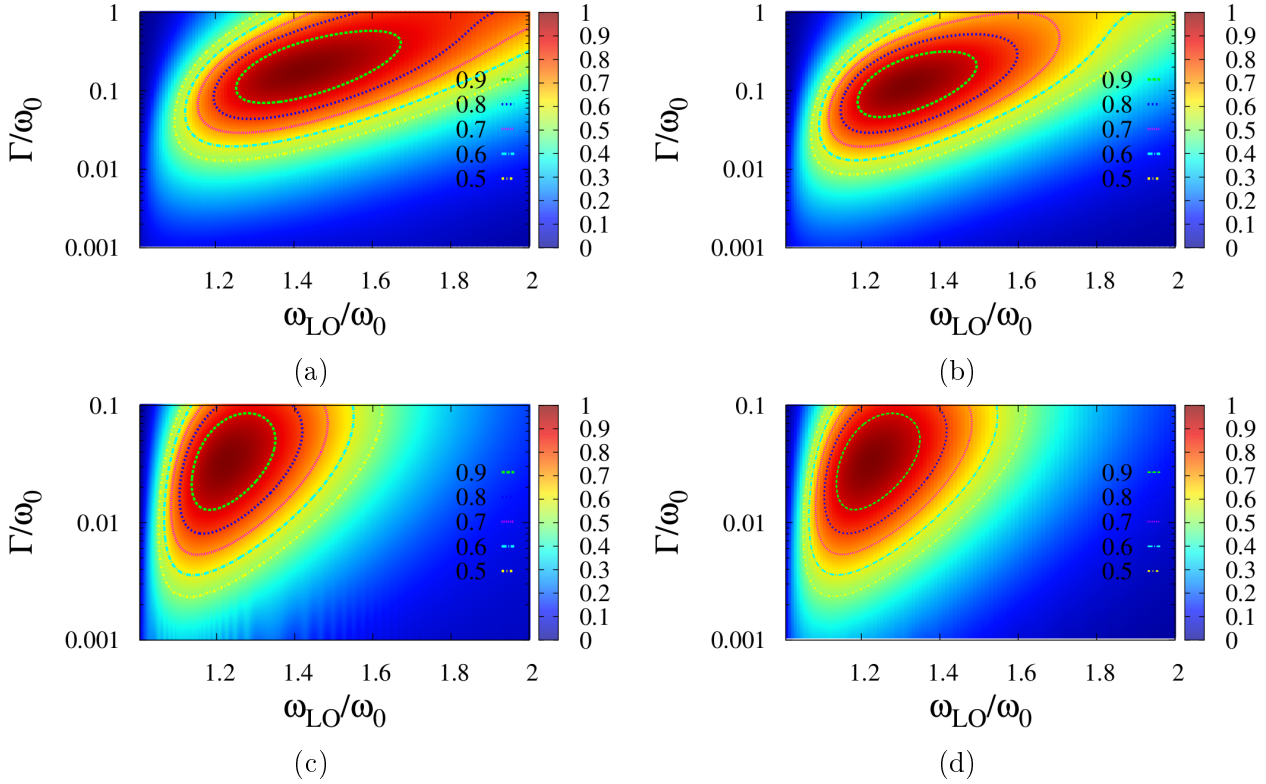

Figure 6: Normalized flux for $\epsilon_\infty = 1$ (a-b) and $\epsilon_\infty = 10$ (c-d) obtained by exact (left column) and approximate (right column) calculation. See Table 3 for a summary of principal relevant results.

Figure 6 presents the normalized NF RHF exchanged by two semi-infinite planes which dielectric permittivities are modeled by Lorentz model for $\epsilon_\infty = 1$ (6a-6b) and $\epsilon_\infty = 10$ (6c-6d) obtained by exact (left column) and asymptotic calculations (right column). Principal relevant results of this figure, concerning the maximum position and value as well as calculation time, are summarized in Table 3.

As for Drude model, we observe the existence of a maximum which is realized by a compromise between the phonons frequencies and the damping factor, i.e. between the peak position and width. For $\epsilon_\infty = 1$ for instance, a maximal flux density $\dot{q}_{max} = 54529$ (W.m^{-2}) is observed at ($\frac{\omega_{LO}}{\omega_{LO}} = 1.42, \frac{\Gamma}{\omega_{TO}} = 1.9 \times 10^{-1}$. Let us note that this $\dot{q}_{max}$ value is almost five times lower than the value obtained with a Drude model at $\epsilon_\infty = 1$ ($\dot{q}_{max} = 229336$). In fact, Drude model is the Lorentz model limit when ω_0 goes zero. Thus, we observe, even though the detailed study of this parameter is not presented in the present paper, an increase of the maximal achievable flux with a Lorentz model when ω_0 decreases. Furthermore, we observe that $\dot{q}_{max}$ sensitivity to ω_{LO} is much larger than to Γ. In fact, the flux is kept at relatively high values ($\dot{q} > 0.9 \times \dot{q}_{max}$) with a relative variation of ω_{LO} around $\pm 12\%$ ($\omega_{LO}/\omega_{TO} \in [1.25, 1.67]$) versus a relative variation of Γ up to $+200\%$ ($\Gamma/\omega_{TO} \in [7 \times 10^{-2}, 5.9 \times 10^{-1}]$).

High frequency limit of the dielectric function effect As for Drude model and for the same reasons, we observe a decrease of $\dot{q}_{max}$ when ϵ_∞ increases in addition to a shift of the

Method	ϵ_∞	$\frac{\omega_{LO}}{\omega_{TO}}$	$\frac{\Gamma}{\omega_{TO}}$	$\dot{q}_{max}$ (W.m^{-2})	$n_{\omega,q}$	$n_{\omega_p,\Gamma}$	t (s)
E	1	1.42	1.9×10^{-1}	56896	2000	100	2.8×10^5
A	1	1.42	1.9×10^{-1}	56905	10000	100	2.51×10^2
E	$\epsilon_{SiC} = 6.7$	1.24	4.78×10^{-2}	14874	4000	100	1.09×10^6
A	$\epsilon_{SiC} = 6.7$	1.24	4.78×10^{-2}	14849	10000	100	1.25×10^2
E	10	1.22	3.31×10^{-2}	10415	3000	100	6.17×10^5
A	10	1.22	3.31×10^{-2}	10391	10000	100	2.5×10^2

Table 3: Optimal Lorentz model parameters for identical media plane-plane configuration. Values are obtained by exact (E) and approximate (A) calculations. $\omega_0 = \omega_{0,SiC} = 1.49 \times 10^{14}$ $rad.s^{-1}$ is kept constant. t is CPU time, $n_{\omega,q}$ and $n_{\omega_p,\Gamma}$ are the mesh points number for frequency and wave vector (ω and q) and control parameters (Γ/ω_0 and ω_{OL}/ω_0) discretization respectively.

maximum position to lower values of ω_{LO}/ω_0 and Γ/ω_0.

Exact versus approximate calculation At this point, Lorentz model strongly contrasts with what was previously observed with Drude model giving very accurate asymptotic results for the maximal flux value as well as for its position. The position relative error is lower than 10^{-3}. Similarly low relative error values are observed for the maximal flux value, except for the case $\epsilon_\infty = 10$ where it reaches 2.3×10^{-3}. Indeed, the maximal flux relative error increases with ϵ_∞, i.e. when $\dot{q}_{max}$ decreases. A part of this error is due to the omission of the propagative contribution in the asymptotic calculation. This contribution is almost constant for different values of ϵ_∞ while the p-polarized evanescent contribution and the total flux decrease when ϵ_∞ increases.
In spite of comparable accuracy, asymptotic calculations are still 1000 times faster than exact ones. In addition, the approximate method shows a better convergence. In fact, some numerical oscillations due to slow convergence can be observed on Figure 6c for small flux values. Calculations performed with higher resolution meshes show that these oscillations magnitude decreases slowly when the mesh points number $n_{\omega,q}$ of $(\omega, \mathbf{q})$ space increases. Thus, we can observe that these oscillations almost disappear on figure 7 obtained with exact calculations, where $n_{\omega,q} = 4000$ and where CPU time is one order of magnitude larger than previously.

Case of silicon carbide at 300 **K** Finally, we consider the case of silicon carbide (SiC). This material has been extensively studied in NF radiative heat transfer literature for its strong surface phonon-polariton resonances around $\omega = 10^{14}$ (rad.s^{-1}).

Figure 7 presents the normalized NF RHF exchanged by two semi-infinite planes modeled by Lorentz model with $\epsilon_\infty = \epsilon_{\infty,SiC} = 6.7$. With only $0.6 \times \dot{q}_{max}$, SiC is far from approaching Lorentz model optimal performances unlike the case of HD-Si which parameters allowed flux values as high as 90% of the maximal RHF that can be obtained with a Drude model when $\epsilon_\infty = \epsilon_{Si}$.

Non-identical media
Now, consider two semi-infinite planes made of non identical materials. We will analyze two cases : (1) the case of SiC and a slightly different material (Figure 8a) (2) The case of the fictive material realizing the optimal performances with $\epsilon_\infty = \epsilon_{\infty,SiC} = 6.7$ (see Table 3, line 3) that we will note material 1 with a slightly different material (Figure 8b). For both cases, $\omega_0 = \omega_{TO,SiC} = 1.49 \times 10^{14}$ $rad.s^{-1}$ is constant. Control parameters are then $\omega_{OL}/\omega_{OL,SiC}$ and Γ/Γ_{SiC} in the first case and $\omega_{OL}/\omega_{OL,1}$ and Γ/Γ_1 in the second.

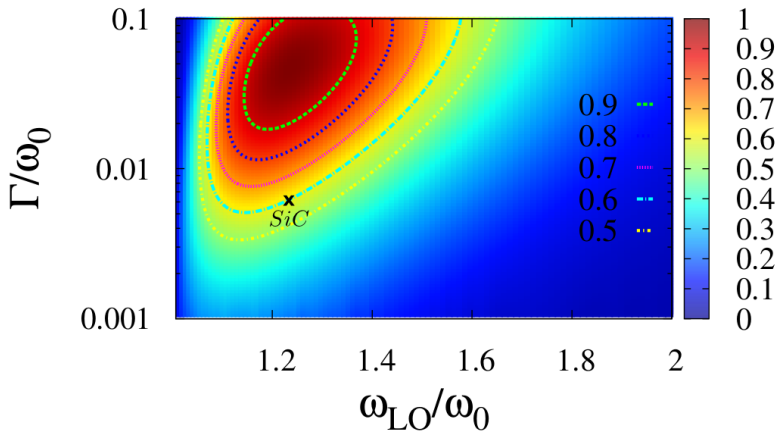

Figure 7: Normalized NF RHF between two semi-infinite planes as a function of $\frac{\omega_{LO}}{\omega_0}$ and $\frac{\Gamma}{\omega_0}$ for $\epsilon_\infty = \epsilon_{\infty,SiC} = 6.7$. SiC parameters values correspond to the point $(1.24, 6\times10^{-3})$[32] indicated by a cross.

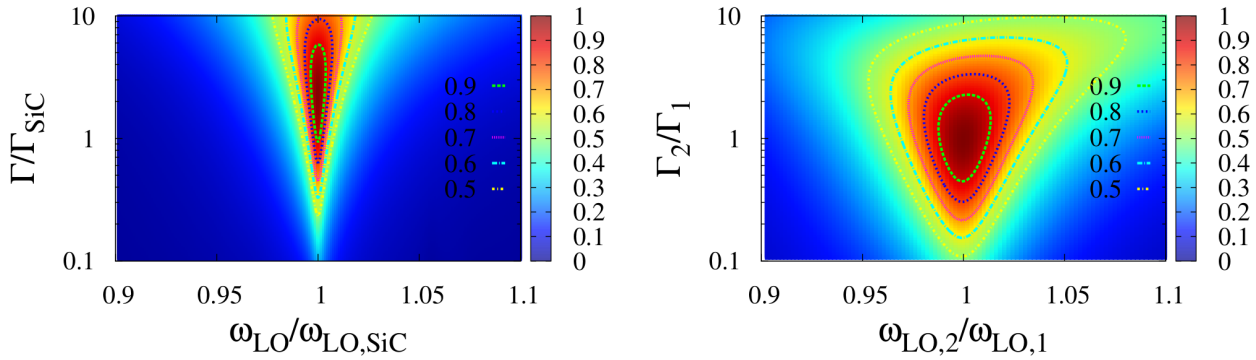

(a) (b)

Figure 8: Normalized NF RHF exchanged by two semi-infinite planes of different non-identical materials which dielectric functions are modeled by Lorentz models. Two cases are considered : (a) SiC exchanging with another material, (b) the material maximizing the transfer between two identical media at $\epsilon_\infty = 6.7$ (see Table 3, line 3) with another material.

Unsurprisingly, the optimum is observed at $(1, 1)$ in both cases, i.e. for identical media. We also observe a high sensitivity, more pronounced for SiC, of the flux to ω_{LO}. In fact, a relative variation of the order of 10^{-4} of ω_{LO} around the point $(1, 1)$ decreases the flux below $0.9 \times \dot{q}_{max}$ while a 8×10^{-3} relative variation of ω_{LO} halves the flux value. $\dot{q}$ is however much less sensitive to Γ since relative variations of this parameter in the range $[-8\%, 581\%]$ maintains $\dot{q} > 0.9 \times \dot{q}_{max}$. The high asymmetry of this range around zero is due to the fact that Γ controls the imaginary part of the dielectric permittivity peak width and height. On the other hand, $\mathrm{Im}(\epsilon)$ controls both emission and absorption. Thus, if Γ increases for the material exchanging with SiC, this material dielectric permittivity imaginary part peak will be wider and lower than SiC's. Therefore, all SiC modes will contribute to the transfer (the new peak is wider than SiC peak), with a lower modes density though (the new peak is lower than SiC peak). Then again, when Γ decreases, the peak becomes narrower and higher than SiC's. All SiC modes do not contribute to the transfer anymore while contributing modes have the same density than in SiC-SiC system. Similar considerations can be made about he second case (Figure 8b) with the only difference that material 1 damping factor is lower than SiC's. This implies a wider peak for $\mathrm{Im}(\epsilon_1)$ which allows looser constraints on the peak position controlled by ω_{LO} and ω_0. For instance, a $\pm1.2\%$ relative variation of ω_{LO} keeps the flux higher than $0.9 \times \dot{q}_{max}$. This value is two orders of

magnitude higher than SiC's, even though it is still relatively small and restrictive in regard to the quality of materials that can be obtained with usual nano-materials deposition techniques.

CONCLUSION

In this work, a study of the effects of different parameters of usual materials local dielectric functions models (Drude and Lorentz) on NF RHF exchanged by two semi-infinite planes separated by a nanometric gap at room temperature is presented. For this purpose, exact and approximate (according to the asymptotic approximation presented in [13]) calculations of the heat flux were calculated. We then showed that the asymptotic approximation leads to highly accurate results, in particular for Lorentz model, with a calculation time at least one thousand times shorter than exact calculation time. Two particular materials usually considered for near-field heat transfer optimization were also considered : silicon carbide (SiC) and highly doped silicon (HD-Si). HD-Si reveals to be well adapted to this aim. In fact, it allows to reach 90% of maximal achievable heat flux by a Drude model with $\epsilon_\infty = 11.8$. It is however possible to overcome these performances by a metamaterial that would have a much lower value of the dielectric permittivity high frequency limit. On the other hand, Lorentz model in general, and SiC in particular, are not the best choice in order to maximize NF radiative heat transfer, at room temperature at least. In addition, SiC is particularly penalizing since its maximal performance is strongly dependent on the quality of used materials. Thus, very small discrepancies, of the order of 10^{-3}, between the phonons frequencies of the two SiC samples would halve the maximal achievable radiative heat flux. We also showed, for both models, that the maximal RHF is obtained when the two semi-infinite planes are made of identical materials. Finally, it is worth mentioning the mesoscopic description of NF radiative heat transfer recently developed [16, 15] and which renews the understanding of this kind of transfer : radiative energy is transported through different modes which have different transmission probabilities from one medium to the other. Total exchanged energy is then obtained by summing the energy of each mode weighed by the mode transmission probability. Maximizing the transfer reduces then to maximizing the transmission probability of the different modes. According to this idea but without performing a detailed optimization study, Ben-Abdallah and Joulain [16] derived with variations calculus a simple analytical condition on Fresnel reflexion coefficients which allows, knowing medium 1, to determine Fresnel coefficients of the second medium maximizing the transfer. It is then possible to determine the optical properties of both media. It would be interesting to implement this method and compare its results and performances to previously presented methods.

ACKNOWLEDGMENTS

Authors would like to thank Philippe Ben-Abdallah and Carsten Henkel for fruitful discussions and gratefully acknowledge the support of the Agence Nationale de la Recherche through the Source-TPV Project No. ANR 2010 BLAN 0928 01.

*

REFERENCES

[1] D. Polder and M. Van Hove, "Theory of radiative heat transfer between closely spaced bodies", *Phys. Rev. B*, vol. 4, pp. 3303–3314, 1971.

[2] E. G. Cravalho, C. L. Tien, and R. P. Caren, "Effect of small spacings on radiative transfer between two dielectrics", *J. Heat Transfer*, vol. 89, no. 4, pp. 351–358, 1967.

[3] E. Rousseau, A. Siria, G. Jourdan, S. Voltz, F. Comin, J. Chevrier, and J-J. Greffet, "Infra-red properties of bulk heavily doped silicon", *Nat. Photon.*, vol. 3, pp. 514, 2009.

[4] A. Kittel, W. Müller-Hirsch, J. Parisi, S-A. Biehs, D. Reddig, and M. Holthaus, "Near-field heat transfer in a scanning thermal microscope", *Phys. Rev. Lett.*, vol. 95, pp. 224301, 2005.

[5] A. Narayanaswamy, S. Shen, and G. Chen, "Near-field radiative heat transfer between a sphere and a substrate", *Phys. Rev. B*, vol. 78, pp. 115303, 2008.

[6] B. Guha, C. Otey, C. B. Poitras, S. Fan, and M. Lipson, "Near-field radiative cooling of nanostructures", *Nano Letters*, vol. 12, no. 9, pp. 4546–4550, 2012.

[7] S. Basu, Z. M. Zhang, and C. J. Fu, "Review of near-field thermal radiation and its application to energy conversion", *Int. J. of Energy Research*, vol. 33, no. 13, pp. 1203–1232, 2009.

[8] M. Francoeur, M. P. Mengüc, and R. Vaillon, "Spectral tuning of near-field radiative heat flux between two thin silicon carbide films", *J. Phys. D: Appl. Phys.*, vol. 43, no. 7, pp. 075501, 2010.

[9] E. Rousseau, M. Laroche, and J-J. Greffet, "Asymptotic expressions describing radiative heat transfer between polar materials from the far-field regime to the nanoscale regime", *J. Appl. Phys.*, vol. 111, no. 1, pp. 014311, 2012.

[10] M. Laroche, R. Carminati, and J.-J. Greffet, "Near-field thermophotovoltaic energy conversion", *J. of Appl. Phys.*, vol. 100, no. 6, pp. 063704, 2006.

[11] M. Francoeur, R. Vaillon, and M.P. Mengüc and, "Thermal impacts on the performance of nanoscale-gap thermophotovoltaic power generators", *Energy Conversion, IEEE Transactions on*, vol. 26, no. 2, pp. 686 –698, june 2011.

[12] S. Basu, B. J. Lee, and Z. M. Zhang, "Near-field radiation calculated with an improved dielectric function model for doped silicon", *J. Heat Trans.*, vol. 132, no. 2, pp. 023302, 2010.

[13] E. Rousseau, M. Laroche, and J.-J. Greffet, "Radiative heat transfer at nanoscale mediated by surface plasmons for highly doped silicon", *Appl. Phys. Lett.*, vol. 95, no. 23, pp. 231913, 2009.

[14] A. I. Volokitin and B. N. J. Persson, "Near-field radiative heat transfer and noncontact friction", *Rev. Mod. Phys.*, vol. 79, pp. 1291–1329, 2007.

[15] S.-A. Biehs, E. Rousseau, and J.-J. Greffet, "Mesoscopic description of radiative heat transfer at the nanoscale", *Phys. Rev. Lett.*, vol. 105, pp. 234301, 2010.

[16] Ph. Ben-Abdallah and K. Joulain, "Fundamental limits for noncontact transfers between two bodies", *Phys. Rev. B*, vol. 82, pp. 121419, 2010.

[17] X. J. Wang, S. Basu, and Z. M. Zhang, "Parametric optimization of dielectric functions for maximizing nanoscale radiative transfer", *J. Phys. D: Appl. Phys.*, vol. 42, no. 24, pp. 245403, 2009.

[18] E. Rousseau, M. Laroche, and J-J. Greffet, "Radiative heat transfer at nanoscale: Closed-form expression for silicon at different doping levels", *J. Quant. Spectrosc. Radiat. Transfer*, vol. 111, no. 7–8, pp. 1005 – 1014, 2010.

[19] M. Abramowitz and I.A. Stegun, *Handbook of Mathematical Functions: With Formulas, Graphs, and Mathematical Tables*, Applied mathematics series. Dover Publ., 1965.

[20] C. Osácar, J. Palacián, and M. Palacios, "Numerical evaluation of the dilogarithm of complex argument", *Celestial Mechanics and Dynamical Astronomy*, vol. 62, pp. 93–98, 1995.

[21] S. Basu, B. J. Lee, and Z. M. Zhang, "Near-field radiation calculated with an improved dielectric function model for doped silicon", *ASME Conference Proceedings*, vol. 2008, no. 48715, pp. 765–772, 2008.

[22] F. Marquier, K. Joulain, J. P. Mulet, R. Carminati, and J. J. Greffet, "Engineering infrared emission properties of silicon in the near field and the far field", *Opt. Commun.*, vol. 237, no. 4-6, pp. 379 – 388, 2004.

[23] E. Nefzaoui, J. Drevillon, and K. Joulain, "Selective emitters design and optimization for thermophotovoltaic applications", *J. Appl. Phys.*, vol. 111, no. 8, pp. 084316, 2012.

[24] S. Basu and Z. M. Zhang, "Maximum energy transfer in near-field thermal radiation at nanometer distances", *J. of Appl. Phys.*, vol. 105, no. 9, pp. 093535, 2009.

[25] V. B. Svetovoy, P. J. van Zwol, and J. Chevrier, "Plasmon enhanced near-field radiative heat transfer for graphene covered dielectrics", *Phys. Rev. B*, vol. 85, pp. 155418, 2012.

[26] R. Messina, J-P. Hugonin, J-J. Greffet, F. Marquier, Y. De Wilde, A. Belarouci, L. Frechette, Y. Cordier, and Ph. Ben-Abdallah, "Tuning the local density of states in graphene-covered systems via strong coupling with graphene plasmons", *eprint arXiv:1211.3145*, 2012.

[27] R. Messina and Ph. Ben-Abdallah, "Graphene-based photovoltaic cells for near-field thermal energy conversion", *eprint arXiv:1207.1476*, 2012.

[28] O. Ilic, M. Jablan, J. D. Joannopoulos, I. Celanovic, and M. Soljacic, "Overcoming the black body limit in plasmonic and graphene near-field thermophotovoltaic systems", *Opt. Express*, vol. 20, no. S3, pp. A366–A384, 2012.

[29] P-O. Chapuis, S. Volz, C. Henkel, K. Joulain, and J-J. Greffet, "Effects of spatial dispersion in near-field radiative heat transfer between two parallel metallic surfaces", *Phys. Rev. B*, vol. 77, pp. 035431, 2008.

[30] Y. Ezzahri, F. Singer, and K. Joulain, "Saturation of near field radiative heat transfer between two polar materials", in *Proceedings of the 7th International Symposium on Radiative Transfer, RAD-13 (submitted).*

[31] A. Borghesi, Chen Chen-Jia, G. Guizzetti, F. Marabelli, L. Nosenzo, E. Reguzzoni, A. Stella, and P. Ostoja, "Infra-red properties of bulk heavily doped silicon", *Il Nuovo Cimento D*, vol. 5, pp. 292–303, 1985.

[32] E. D. Palik, *Handbook of Optical Constants of Solids*, Academic Press, Boston, 1985.